Measuring neutron-star properties via gravitational waves from binary mergers

A. Bauswein[1] and H.-T. Janka[1]

[1] *Max-Planck-Institut für Astrophysik, Karl-Schwarzschild-Str. 1, D-85748 Garching, Germany*

(Dated: June 9, 2011)

We demonstrate by a large set of merger simulations for symmetric binary neutron stars (NSs) that there is a tight correlation between the frequency peak of the postmerger gravitational-wave (GW) emission and the physical properties of the nuclear equation of state (EoS), e.g. expressed by the radius of the maximum-mass Tolman-Oppenheimer-Volkhoff configuration. Therefore, a single measurement of the peak frequency of the postmerger GW signal will constrain the NS EoS significantly. For plausible optimistic merger-rate estimates a corresponding detection with Advanced LIGO is likely to happen within an operation time of roughly a year.

PACS numbers: 04.30.Db,26.60.Kp,95.85.Sz,97.60.Jd

The properties of high-density matter as in the cores of NSs, in particular the EoS, are still incompletely known, because the physical conditions are not directly accessible by experiments. Theoretical models for supernuclear matter are ambiguous and suffer from uncertainties of nuclear data required as input for these calculations [1].

NS properties are intimately linked to the adopted EoS because the latter determines stellar structure through the Tolman-Oppenheimer-Volkhoff (TOV) equations [1, 2]. Hence, constraints on the NS EoS can be deduced from astrophysical observations (e.g. [3]), as alternatives to nuclear models [4] and laboratory experiments (see [2] for a review).

NS mergers may also yield information about the nuclear EoS, because the dynamics of the coalescence depend sensitively on the behavior of high-density matter (see [5, 6] for a review). Consequently, the EoS leaves an imprint on the GW signal of NS mergers. However, the systematic dependences of the inverse problem, i.e. which EoS (or NS) properties can be derived from a particular GW detection, are still not completely explored (see [5, 7–15] and refs. therein). In this letter we report on a tight correlation between NS parameter and thus EoS characteristics and the dominant frequency of the postmerger GW emission revealed by a systematic study with 19 microphysical EoSs. Our survey is in particular important, because the second-generation interferometric GW detectors of Advanced LIGO [16] and Advanced Virgo [17] go into operation within the next years. NS binaries are considered a major target of these instruments with an estimated detection rate of 0.4 to 400/yr [18].

Our simulations are performed with a 3-D relativistic smoothed particle hydrodynamics (SPH) code [19, 20], which solves the Einstein field equations assuming conformal flatness. The implementation allows the usage of tabulated microphysical EoSs including thermal effects, or arbitrary barotropic EoSs (e.g. zero-temperature EoSs for matter in equilibrium to weak interactions, the so-called β-equilibrium). The latter are supplemented by an ideal-gas component with an ideal-gas index $\Gamma_{\rm th} = 2$ to mimic thermal effects [21].

The calculations start from quasi-equilibrium orbits about two revolutions before the merging of the NSs, which are assumed to be initially cold and in neutrinoless β-equilibrium. The stars are set up with an irrotational velocity profile. If not noted otherwise the NSs are modeled by about 340,000 SPH particles.

In total we employ 19 different microphysical EoSs (see Tab. I for the nomenclature and references). Seven of these EoSs include thermal effects consistently. The remaining ones describe nuclear matter at zero temperature and are labeled with "$+\Gamma_{\rm th}$" in Tab. I. The MIT60 EoS models selfbound strange quark matter (SQM; see e.g. [1, 20, 22] for this case).

The mass-radius (M-R) relations, the maximum masses $M_{\rm max}$ of non-rotating NSs and the corresponding (minimum) radii, denoted as $R_{\rm max}$, for all employed EoSs are shown in Fig. 1. The maximum-mass configurations (Tab. I) are marked by symbols. The scatter in Fig. 1 illustrates the diversity of the underlying microphysical models of our study.

We consider EoSs with $M_{\rm max}$ in the range of 1.80 $M_\odot$ to 2.76 $M_\odot$ and $R_{\rm max}$ from 9.30 km to 14.30 km without any special selection procedure except that we require $M_{\rm max} \geq 1.8\ M_\odot$. The lower limit of 1.8 $M_\odot$ is motivated by the detection of a pulsar with a mass of $(1.97 \pm 0.04)\ M_\odot$ [3]. Although this observation rules out some EoSs of our sample, we do not disregard these models, because at lower densities (as present in 1.35 $M_\odot$ NSs and in the merger remnant where strong rotational and thermal effects come into play) these EoSs may still provide a viable description of nuclear matter. Furthermore, the inclusion of these EoSs demonstrates the validity of the relations between merger and EoS properties discussed below over a wider parameter range.

For each EoS listed in Tab. I we simulate the merger of two stars with 1.35 $M_\odot$. This setup is chosen because pulsar observations [39] and population synthesis studies [40] suggest these systems to be most abundant.

After energy and angular momentum losses by GWs have driven the inspiral of the NSs for several 100 Myrs, there are different outcomes of the coalescence. Either

TABLE I: Used EoSs with references. $M_{\rm max}$ and $R_{\rm max}$ are the gravitational mass and radius of the maximum-mass TOV configurations, $f_{\rm peak}$ is the dominant frequency of the postmerger GW emission (a cross indicates prompt collapse of the merger remnant). The tables of the first five and next seven EoSs are taken from [23] and [24], respectively.

EoS	$M_{\rm max}$ [$M_\odot$]	$R_{\rm max}$ [km]	$f_{\rm peak}$ [kHz]
Sly4 [25] $+\Gamma_{\rm th}$	2.05	10.01	3.32
APR [26] $+\Gamma_{\rm th}$	2.19	9.90	3.46
FPS [27] $+\Gamma_{\rm th}$	1.80	9.30	x
BBB2 [28] $+\Gamma_{\rm th}$	1.92	9.55	3.73
Glendnh3 [29] $+\Gamma_{\rm th}$	1.96	11.48	2.33
eosAU [30] $+\Gamma_{\rm th}$	2.14	9.45	x
eosC [31] $+\Gamma_{\rm th}$	1.87	9.89	3.33
eosL [32] $+\Gamma_{\rm th}$	2.76	14.30	1.84
eosO [33] $+\Gamma_{\rm th}$	2.39	11.56	2.66
eosUU [30] $+\Gamma_{\rm th}$	2.21	9.84	3.50
eosWS [30] $+\Gamma_{\rm th}$	1.85	9.58	x
SKA [34] $+\Gamma_{\rm th}$	2.21	11.17	2.64
Shen [35]	2.24	12.63	2.19
LS180 [34]	1.83	10.04	3.26
LS220 [34]	2.04	10.61	2.89
LS375 [34]	2.71	12.34	2.40
GS1 [36]	2.75	13.27	2.10
GS2 [37]	2.09	11.78	2.53
MIT60 [38]	1.88	10.35	3.43

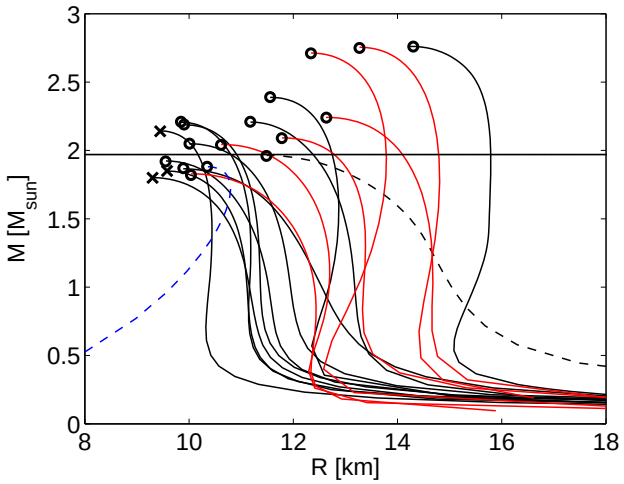

FIG. 1: NS M-R relations for all considered EoSs. Red curves correspond to EoSs that include thermal effects consistently, black lines indicate EoSs supplemented with a thermal ideal gas, the SQM EoS MIT60 is displayed in blue. The horizontal line corresponds to the observed 1.97 $M_\odot$ NS [3].

the two stars directly form a black hole (BH) shortly after they fuse ("prompt collapse"), or the merging leads to the formation of a differentially rotating object (DRO) that is stabilized against the gravitational collapse by rotation and thermal pressure contributions emerging from compression and shock heating during the collision. Continuous loss of angular momentum by GWs and redistribution to the outer merger remnant will finally lead to a "delayed collapse" on timescales of typically several 10–100 ms depending on the mass and the EoS. For EoSs with a sufficiently high $M_{\rm max}$ stable or very long-lived rigidly rotating NSs are the final product.

A prompt collapse occurs for three EoSs of our sample (marked by x in Tab. I and Fig. 1). One observes this scenario only for EoSs with small $R_{\rm max}$. In the simulations with the remaining EoSs DROs are formed. The evolution of these mergers is qualitatively similar. Details of the dynamics of the coalescence, in particular the formation of spiral arms and torus-like structures around the central merger remnant are described in [19, 20].

For all models that produce a DRO the GW signal is analyzed by a post-Newtonian quadrupole formula [19]. The inset of Fig. 2 shows the GW amplitude of the plus polarization at a polar distance of 50 Mpc for NSs described by the Shen EoS. Clearly visible is the inspiral phase with an increasing amplitude and frequency (until 5 ms), followed by the merging and the ringdown of the postmerger remnant (from 6 ms). In Fig. 2 the scaled power spectral density $h_+(f)\sqrt{f}$ with the Fourier transformed waveform $h_+(f)$ is given for the Shen EoS (black) and eosUU (blue) assuming optimal orientation of source at 50 Mpc and detector together with the anticipated sensitivity for Advanced LIGO [16] and the planned Einstein Telescope (ET) [41]. As a characteristic feature of the spectrum a pronounced peak at $f_{\rm peak} = 2.19$ kHz for the Shen EoS and 3.50 kHz for eosUU is found, which is known to be connected to the GW emission of the merger remnant [7]. Recently, this peak has been identified as the frequency of the fundamental quadrupolar fluid mode (f-mode) [42]. The peak in the kHz range is generic for all mergers producing a DRO and it has been estimated to be measurable with Advanced LIGO out to $\sim$35 Mpc [11] or even $\sim$50 Mpc [13]. Values of $f_{\rm peak}$ for all our models are listed in Tab. I. Higher resolved runs with 550,000 and 1,270,000 SPH particles confirm that $f_{\rm peak}$ is determined to an accuracy of about one per cent. Furthermore, our $f_{\rm peak}$ values agree within a few per cent with the results of fully relativistic simulations (e.g. 3.35 kHz for the APR EoS in [10]; the prompt collapse for the FPS EoS has been confirmed in [9]). The uncertainties associated with the $\Gamma_{\rm th}-$ansatz for thermal effects are below 10 per cent [21].

Our systematic study reveals that the peak frequency $f_{\rm peak}$ of the postmerger GW signal and characteristic NS properties are closely related. In Fig. 3 $f_{\rm peak}$ is plotted against $R_{\rm max}$ (crosses and triangles) and an obvious correlation between these two quantities is visible. The peak frequency is higher for smaller $R_{\rm max}$ with a slight change of the slope around 11 km. The two outliers (trian-

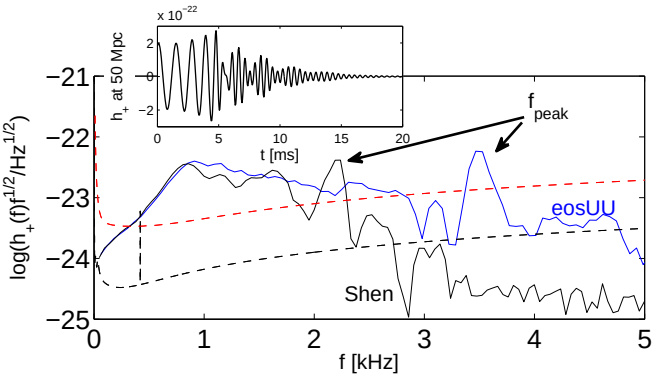

FIG. 2: Scaled power spectral density of the GW signal for the Shen (black solid line) and the eosUU (blue line) EoSs compared to the Advanced LIGO (red dashed line) and ET (black dashed line) unity SNR sensitivities. The inset shows the GW amplitude of the + polarization at 50 Mpc for the Shen EoS.

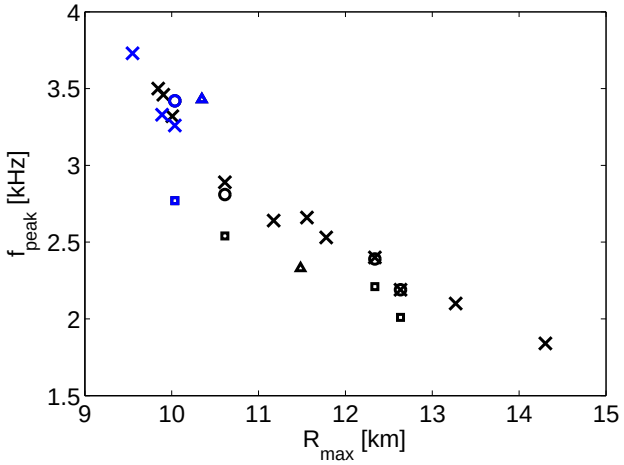

FIG. 3: Peak frequency of the postmerger GW emission vs. radius of the maximum-mass TOV solution. Blue cases are excluded by [3]. See text for symbols.

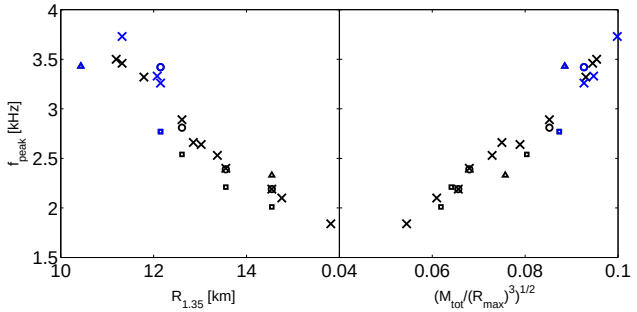

FIG. 4: Peak frequency vs. radius of a 1.35 $M_\odot$ NS (left) and vs. $\sqrt{M_{\rm tot}/R_{\rm max}^3}$ in geometrical units (right) with $M_{\rm tot}$ being the binary mass. Symbols have same meaning as in Fig. 3.

gles) belong to simulations for the MIT60 and Glendnh3 EoSs, which both have strikingly different M-R relations (dashed lines in Fig. 1). Note that a SQM EoS could lead to discriminating observational features, e.g. in the cosmic ray flux [20, 22], but the particular model MIT60 is ruled out by the 1.97 $M_\odot$ NS of [3]. The Glendnh3 EoS seems in conflict with theoretical knowledge of EoS properties at subnuclear densities [4]. Ignoring the two outliers, the $f_{\rm peak} - R_{\rm max}$ correlation (crosses only) becomes even stronger. Already one determination of $f_{\rm peak}$ could therefore seriously constrain the M-R relation and consequently the nuclear EoS. Additionally, simulated mergers of 1.2 $M_\odot$-1.5 $M_\odot$ binaries for selected EoSs (circles) demonstrate that the relation between $f_{\rm peak}$ and $R_{\rm max}$ is not very sensitive to the initial mass ratio [11]. Squares in Fig. 3 display results for 1.2 $M_\odot$-1.2 $M_\odot$ mergers. For those $f_{\rm peak}$ is clearly lower [11] with differences being larger for smaller $R_{\rm max}$. But also for the symmetric binaries with lower mass a correlation seems to exist. We stress that the total binary mass $M_{\rm tot}$ will be measurable by the GW inspiral signal [43].

$f_{\rm peak}$ turns out to correlate also with other NS properties: From Fig. 4 (left panel) a close relation between the radius $R_{1.35}$ of a 1.35 $M_\odot$ star (or alternatively its compactness $GM/(c^2R)$) and $f_{\rm peak}$ is evident. Again only the MIT60 and Glendnh3 EoSs occur as outliers. This finding is not surprising, because the TOV solutions show already an approximate correlation between $R_{1.35}$ and $R_{\rm max}$. A similar coupling is found between $f_{\rm peak}$ and the maximum central density $\rho_{\rm max}$ of non-rotating NSs, where higher $\rho_{\rm max}$ yield higher $f_{\rm peak}$.

However, no clear correlation exists between $f_{\rm peak}$ and the maximum compactness of non-spinning NSs or $M_{\rm max}$, though typically a lower $M_{\rm max}$ gives a higher $f_{\rm peak}$, and $f_{\rm peak} > 2.8$ kHz seems incompatible with $M_{\rm max} > 2.4\ M_\odot$. We propose the following explanation for the fact that the postmerger GW emission is determined by $R_{\rm max}$. Numerical calculations have shown that for any EoS the frequency of the f-mode, which generates the GW radiation at $f_{\rm peak}$ [42], depends nearly linearly on the square root of the mean density $(M/R^3)^{1/2}$ [44]. Since we fix $M_{\rm tot}$, the mass-dependence drops out. Assuming that the radius of the DRO relates to the M-R relation of non-rotating NSs [47], we end up with $f_{\rm peak} \propto R_{\rm max}^{-1.5}$. This hypothesis is verified in the right panel of Fig. 4, where $f_{\rm peak}$ is plotted versus $(M_{\rm tot}/R_{\rm max}^3)^{1/2}$ and except for the mentioned outliers a clear power-law scaling is visible.

Despite an estimated detection rate of only 0.1 to 1 events/yr for Advanced LIGO (accounting for random orientation and adopting the "realistic" and the "high" merger rates of [18]) the relations found in this work may prove very useful, because already a single measurement is likely to determine $R_{\rm max}$ and $R_{1.35}$ to within some 100 m. This will place significant constraints on the M-R relation and thus the EoS (see [2, 45] for the inverse procedure). These prospects appear superior to the

1 km accuracy of the radius estimation for the initial NSs from the inspiral GW signal of symmetric binaries suggested in [12] for events within a maximal distance of 20–100 Mpc, assuming optimal source orientation. Furthermore, only a weak correlation exists between $M_{\rm max}$ and the threshold total binary mass $M_{\rm thres}$ that distinguishes prompt ($M_{\rm tot} > M_{\rm thres}$) and delayed ($M_{\rm tot} < M_{\rm thres}$) BH formation [15], and the determination of $M_{\rm thres}$ requires more than one GW detection [13]. Therefore, our finding provides a unique possibility to probe the very high-density regime hard to explore by other astrophysical methods also because of the rare observations of very massive NSs close to $M_{\rm max}$. Moreover, the planned ET [41] will have an increased sensitivity making several observations of $f_{\rm peak}$ per year very likely.

Future investigations should vary $M_{\rm tot}$ and confirm our findings by more sophisticated models of binary mergers, e.g. taking into account magnetic fields, neutrino physics and full general relativity. Also the capabilities of data analysis to measure $f_{\rm peak}$ e.g. in a detector network, should be explored. Finally, our explanation should be examined in more detail to develop an understanding of the presented correlations.

We thank N. Stergioulas, D. Shoemaker and S. Hild. This work was supported by DFG grants SFB/TR 7, SFB/TR 27, EXC 153, by ESF/CompStar, and by computer time at LRZ Munich, RZG Garching and MPA Garching.

[1] P. Haensel, A. Y. Potekhin, and D. G. Yakovlev, *Neutron Stars 1* (Springer-Verlag, New York, 2007).
[2] J. M. Lattimer and M. Prakash, Phys. Rep. **442**, 109 (2007).
[3] P. B. Demorest, T. Pennucci, S. M. Ransom, M. S. E. Roberts, and J. W. T. Hessels, Nature (London) **467**, 1081 (2010).
[4] K. Hebeler, J. M. Lattimer, C. J. Pethick, and A. Schwenk, Phys. Rev. Lett. **105**, 161102 (2010).
[5] M. D. Duez, Class. Quantum Grav. **27**, 114002 (2010).
[6] J. Faber, Class. Quantum Grav. **26**, 114004 (2009).
[7] X. Zhuge, J. M. Centrella, and S. L. W. McMillan, Phys. Rev. D **50**, 6247 (1994).
[8] J. A. Faber, P. Grandclément, F. A. Rasio, and K. Taniguchi, Phys. Rev. Lett. **89**, 231102 (2002).
[9] M. Shibata, K. Taniguchi, and K. Uryū, Phys. Rev. D **71**, 084021 (2005).
[10] M. Shibata and K. Taniguchi, Phys. Rev. D **73**, 064027 (2006).
[11] R. Oechslin and H.-T. Janka, Phys. Rev. Lett. **99**, 121102 (2007).
[12] J. S. Read, C. Markakis, M. Shibata, K. Uryū, J. D. E. Creighton, and J. L. Friedman, Phys. Rev. D **79**, 124033 (2009).
[13] M. Shibata, Phys. Rev. Lett. **94**, 201101 (2005).
[14] L. Baiotti, T. Damour, B. Giacomazzo, A. Nagar, and L. Rezzolla, Phys. Rev. Lett. **105**, 261101 (2010).
[15] K. Hotokezaka, K. Kyutoku, H. Okawa, M. Shibata, and K. Kiuchi, ArXiv e-prints (2011), 1105.4370.
[16] G. M. Harry and the LIGO Scientific Collaboration, Class. Quantum Grav. **27**, 084006 (2010).
[17] F. Acernese et al., Class. Quantum Grav. **23**, S635 (2006).
[18] J. Abadie et al., Class. Quantum Grav. **27**, 173001 (2010).
[19] R. Oechslin, H.-T. Janka, and A. Marek, Astron. Astrophys. **467**, 395 (2007).
[20] A. Bauswein, R. Oechslin, and H.-T. Janka, Phys. Rev. D **81**, 024012 (2010).
[21] A. Bauswein, H.-T. Janka, and R. Oechslin, Phys. Rev. D **82**, 084043 (2010).
[22] A. Bauswein, H.-T. Janka, R. Oechslin, G. Pagliara, I. Sagert, J. Schaffner-Bielich, M. M. Hohle, and R. Neuhäuser, Phys. Rev. Lett. **103**, 011101 (2009).
[23] www.lorene.obspm.fr.
[24] www.gravity.phys.uwm.edu/rns.
[25] F. Douchin and P. Haensel, Astron. Astrophys. **380**, 151 (2001).
[26] A. Akmal, V. R. Pandharipande, and D. G. Ravenhall, Phys. Rev. C **58**, 1804 (1998).
[27] B. Friedman and V. R. Pandharipande, Nucl. Phys. A **361**, 502 (1981).
[28] M. Baldo, I. Bombaci, and G. F. Burgio, Astron. Astrophys. **328**, 274 (1997).
[29] N. K. Glendenning, Astrophys. J. **293**, 470 (1985).
[30] R. B. Wiringa, V. Fiks, and A. Fabrocini, Phys. Rev. C **38**, 1010 (1988).
[31] H. A. Bethe and M. B. Johnson, Nucl. Phys. A **230**, 1 (1974).
[32] V. R. Pandharipande and R. A. Smith, Phys. Lett. B **59**, 15 (1975).
[33] R. L. Bowers, A. M. Gleeson, and R. Daryl Pedigo, Phys. Rev. D **12**, 3043 (1975).
[34] J. M. Lattimer and F. D. Swesty, Nucl. Phys. A **535**, 331 (1991).
[35] H. Shen, H. Toki, K. Oyamatsu, and K. Sumiyoshi, Nucl. Phys. A **637**, 435 (1998).
[36] G. Shen, C. J. Horowitz, and S. Teige, Phys. Rev. C **83**, 035802 (2011).
[37] G. Shen, C. J. Horowitz, and E. O'Connor, ArXiv e-prints (2011), 1103.5174.
[38] EoS provided by G. Pagliara, I. Sagert (details in [20]).
[39] S. E. Thorsett and D. Chakrabarty, Astrophys. J. **512**, 288 (1999).
[40] K. Belczynski, R. O'Shaughnessy, V. Kalogera, F. Rasio, R. E. Taam, and T. Bulik, Astrophys. J. Lett. **680**, L129 (2008).
[41] S. Hild, S. Chelkowski, A. Freise, J. Franc, N. Morgado, R. Flaminio, and R. DeSalvo, Class. Quantum Grav. **27**, 015003 (2010).
[42] N. Stergioulas, A. Bauswein, K. Zagkouris, and H.-T. Janka, ArXiv e-prints (2011), 1105.0368.
[43] C. Cutler and É. E. Flanagan, Phys. Rev. D **49**, 2658 (1994).
[44] N. Andersson and K. D. Kokkotas, Mon. Not. R. Astron. Soc. **299**, 1059 (1998).
[45] L. Lindblom, Astrophys. J. **398**, 569 (1992).
[46] J.-P. Lasota, P. Haensel, and M. A. Abramowicz, Astrophys. J. **456**, 300 (1996).
[47] This assumption is supported by the empirical finding

that for any EoS the radius of the most massive, rigidly rotating NS is correlated with $R_{\rm max}$ [46], and thus also with $R_{1.35}$. This suggests a similar connection for a differentially rotating NS with 2.7 $M_\odot$.